

Surface shape measurements exploiting the moire effect of colour CCD image sensor

W. PARA, W. ŚMIETAŃSKI

Electromechanical Faculty, Technical Military Academy, ul. Kaliskiego, 00-908 Warszawa, Poland.

In the article, a method of surface shape measurement based on specific periodic structure of the colour CCD image sensor has been proposed. Theoretical apparatus of the discrete phase change method has been exploited to the analysis of fringe images. Three moire fringe images shifted in phase are obtained simultaneously as a result of image sampling with the help of a colour CCD image sensor equipped with a colour vertical stripe filter. Both theoretical analysis and experimental results have been presented.

1. Introduction

A quick development of the methods of the surface shape measurements has been observed for over ten years. This is due to urgent request for information on surface geometry in such fields as: surface quality control, robotics, objects recognition, medical diagnostics, computer-aided design and other industrial applications. One of the most rapidly developing groups of measurement methods are touchless optical technics offering both high accuracy and rate of measurements. Many optical methods of surface geometry measurements applying both passive and active technics have been proposed. The active technics, such as triangulation, moire methods, holographic methods, measurements of distance by impuls methods, have found wide application in practice. An extensive survey of optical technics has been presented in [1].

The moire methods have been commonly used for precision measurements of the surface geometry for many years. In the projection moire method, a projection of transmission profile of rectangular wave type (Ronchi grating) is made on the surface under test. If this surface is not plane, the lines of projection network seen through an identical detection network are no more straight lines, which consequently results in creation of a moire fringe image. In the systems exploiting the CCD cameras, it is possible to obtain the moire fringe images by using the periodical structure of CCD image sensor instead of detection network [2].

The information concerning the shape of the surface of the examined object may be recovered on the basis of the measurements of the fringe image phase. Many methods have been worked out enabling the phase measurements in the fringe images on the basis of their automatic analysis [3].

One of the most popular methods of automatic analysis of fringe images is that of the discrete change of phase. In this method, the phase measurement is performed on the basis of analysis of, at least, three fringe images shifted mutually in phase.

The change of phase in images is usually achieved by shifting the projection network. The basic advantage offered by this method is simplicity of calculations required to recover the shape of the examined surface, while its disadvantage lies in necessity of applying high-precision systems for shifting the projection network. Moreover, the method of discrete change of phase requires stable position of the examined object during recording of the subsequent fringe images shifted in phase. In many practical applications, both industrial and medical, this last fact makes the usage of this method, either excluded or significantly reduced due to low measurement accuracy.

The methods of surface geometry measurements suggested in [4], [5] are free of the said disadvantages of the method of discrete change of phase. In these systems, the colour projection network is applied which is obtained by superposing three sinusoids shifted in phase in each of fundamental RGB colours. This eliminates the necessity of precision positioning of the projection network, because the phase shifts between the fringe images are determined in the production process of such networks. Simultaneous recording of three fringe images shifted in phase is assured by the colour camera.

The measurement technique of surface geometry proposed in this paper is based on the projection of the black-and-white projection network onto the surface of the examined object and recording of the three moire fringe images shifted in phase and produced in three colour channels of the CCD camera, each corresponding to one fundamental colour. The phase shift between particular fringe images is obtained by using specific periodical structure of the CCD image sensor with time splitting of signals and colour strip filter.

2. Image sampling

2.1. Image sampling by monochromatic image sensor

Let us consider the sampling process of the $G(x)$ image with periodical intensity distribution by one line of light-sensitive elements of a monochromatic CCD image sensor. The geometry of such line is characterized by its total length B , the width of the photosensitive region of singular pixel b , and the distance d between the

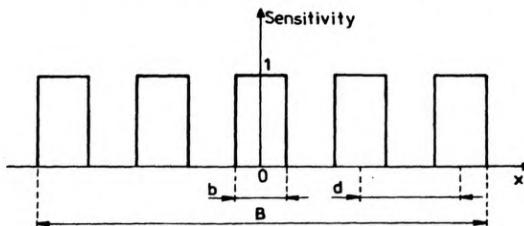


Fig. 1. Model of the normalized photosensitivity of the CCD image sensor

neighbouring pixels (Fig. 1). The output signal $G_s(x)$ of the image sensor may be written as [2], [6]

$$G_s(x) = \left[G(x) * \frac{1}{b} \text{rect} \left(\frac{x}{b} \right) \right] \frac{1}{d} \text{comb} \left(\frac{x}{d} \right) \text{rect} \left(\frac{x}{B} \right) \quad (1)$$

where $*$ denotes the convolution operation.

The Fourier transform of the signal (1) has the form

$$G_s(f) = [G(f) \text{sinc}(bf)] * \text{comb}(df) * B \text{sinc}(Bf) \quad (2)$$

where $G(f)$ is the Fourier transform of the image $G(x)$. Consider the sampling of an image of periodical form

$$G(x) = \frac{1}{2} \{1 + \cos[2\pi f_g x + \Phi(x)]\} \quad (3)$$

where: f_g – image frequency,

$\Phi(x)$ – image phase modulation.

If the spectrum of distribution $\Phi(x)$ has a limited maximal pulsation, then the principal spectral power of the image (3) is also concentrated within a limited band [8]. An example of spectrum $G_{f_g}(f)$ of effective bandwidth B_B for the image (3) of frequency f_g is shown in Fig. 2a.

When sampling the image (3), the output signal of the image sensor, obtained by convolving the spectrum $G_{f_g}(f)$ with the $\text{comb}(df)$ function (Fig. 2b) takes the spectrum of the form

$$G_s(f) = \left\{ \sum_{m=-\infty}^{\infty} G_{f_g} \left[f - \frac{m}{d} \right] \text{sinc} \left[b \left(f - \frac{m}{d} \right) \right] \right\} * B \text{sinc}(Bf) \quad (4)$$

presented in Fig. 2c for the case $f_g < f_n$, where $f_n = 1/(2d)$ is the Nyquist frequency of the image sensor. If the image frequency is higher than the Nyquist frequency of the image sensor ($f_g > f_n$), the output signal spectrum takes the form presented in Fig. 2d.

Taking account of the fact that in the output signal of the transducer only components of frequencies lower than Nyquist frequency may be observed, the spectrum presented in Fig. 2d may be interpreted as a result of convolution of the $\text{comb}(df)$ function with the spectrum $G_{2f_n - f_g}(f)$ which is presented in Fig. 2e. As a result of this convolution, we obtain

$$G_s(f) = \left\{ G_{2f_n - f_g}(f) \text{sinc}[b(f - 2f_n)] \right\} * \text{comb}(df) * B \text{sinc}(Bf) \quad (5)$$

which, after performing the inverse Fourier transform, allows us to obtain the relation for output signal of the image sensor

$$G_s(x) = \{A(x) + B(x) \cos[2\pi(2f_n - f_g)x + \Phi(x)]\} \frac{1}{d} \text{comb} \left[\frac{x}{d} \right] \text{rect} \left[\frac{x}{B} \right] \quad (6)$$

representing the fringe image of frequency $2f_n - f_g$. The changes of both the d.c. component $A(x)$ and the amplitude $B(x)$ follow from averaging of the signal over the pixel area.

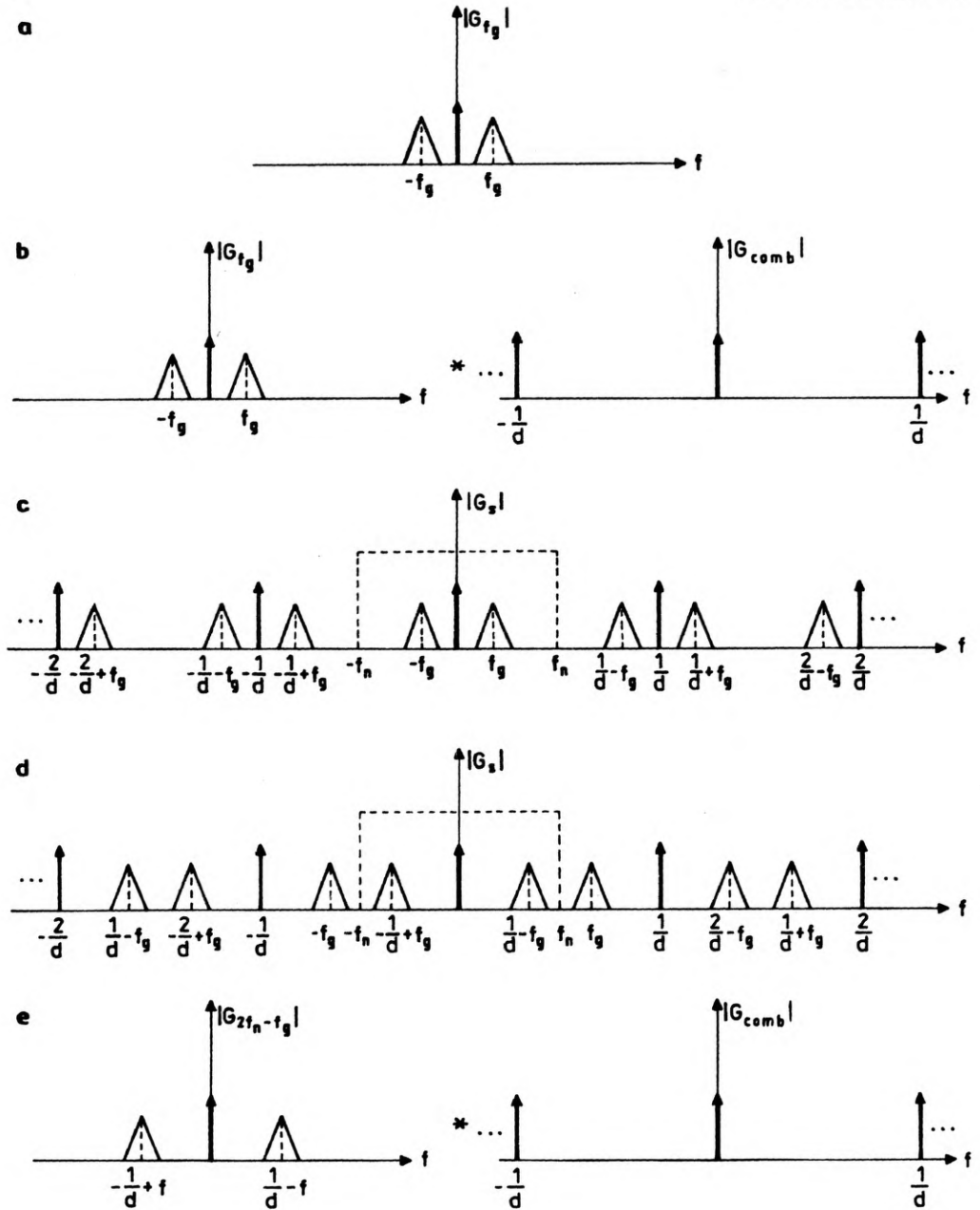


Fig. 2. Example of spectrum of the periodic image — a, creation of the output signal spectrum of the image sensor due to convolution of the image spectrum with the $\text{comb}(df)$ function — b, output signal spectrum of the image sensor for $f_g < f_n$ — c, output signal spectrum of the image sensor for $f_g > f_n$ — d, new component of the output signal frequency of the image sensor resulting from the spectrum superposition — e

2.2. Single-chip colour CCD camera

Trichromatic analysis of the colour image may be performed by using only one image sensor [7]. The basic element of the single-chip camera is, beside an arbitrary analysing image sensor, a colour filter. This is an optical element of discontinuous structure, the spectral transmission properties of which depend upon the place of light flux incidence. The colour filter is usually an integral part of the analysing transducer — both subassemblies being produced simultaneously.

Image analysis in the single-chip colour camera proceeds as follows: the light flux is projected by optical system via colour filter onto the photosensitive surface of the image sensor. The electric signals appearing in the image sensor structure corresponding to the analysed image transformed by the filter are next read out in the way appropriate for the given type of image sensor. The obtained output distributions (runs) serve to form three electric signals in the electric part of the camera corresponding to fundamental colours of the analysed image.

The fidelity of the colour image analysis performed in the single-chip camera depends strongly on the applied colour filter. One of the applied structures of this filter is stripe filter (Fig. 3). The widths of the elements of the stripe filter are equal to the widths of the photosensitive elements of the applied image sensor.

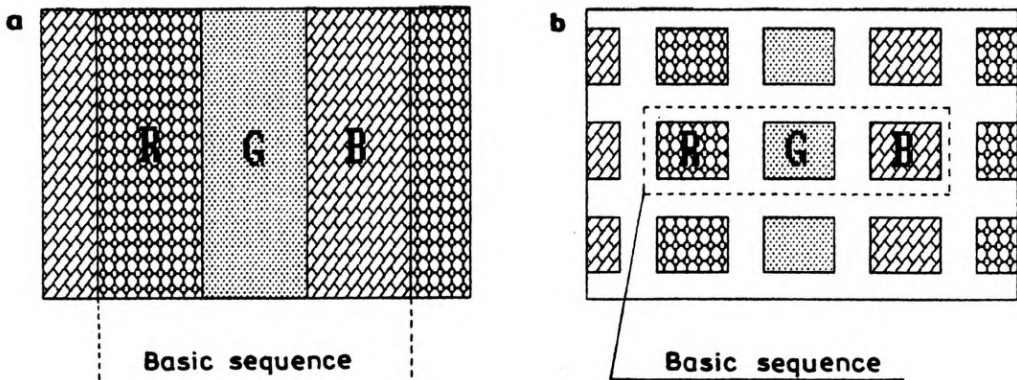


Fig. 3. Structure of the primary colour stripe filter: a — continuous, b — mozaic

Colour elements of limited surface of the stripe filter lead the filtered light to precisely determined, mutually separated and always the same photosensitive elements. The quantity of the charge collected inside a certain photosensitive region is thus proportional to the value of the fundamental colour signal transmitted by the element of the colour filter connected with this region. This means that the information about the signal of each fundamental colour is not collected in all the photosensitive elements of image sensor.

For primary colour vertical stripe filter (its fundamental colours being RGB), the signal of each fundamental colour is created by interpolation of the charge value (electric signal) collected in every third photosensitive element of the colour

image sensor equipped with this type of filter. The Nyquist frequency f_{nk} for each channel of the image sensor is thus three times lower than the Nyquist frequency of the image sensor of identical geometry of the photosensitive element working without colour filter

$$f_{nk} = f_n/3. \quad (7)$$

2.3. Output signal of the single-chip colour camera with the time splitting of signals

From the principle of image analysis described in subsection 2.2, by using the image sensor equipped with primary colour stripe filter, it follows that three components corresponding to the transmission bands of the RGB filter elements may be distinguished in the image sensor output signal. If the output signal of the image sensor takes the form of a diffused image of the projection network projected on the examined surface, the intensity distributions of these components may be represented as:

$$\begin{aligned} G_R(x) &= a_{0R}(x) + a_{1R}(x) \cos [2\pi f_g x + \Phi(x)], \\ G_G(x) &= a_{0G}(x) + a_{1G}(x) \cos [2\pi f_g x + \Phi(x)], \\ G_B(x) &= a_{0B}(x) + a_{1B}(x) \cos [2\pi f_g x + \Phi(x)] \end{aligned} \quad (8)$$

where $\Phi(x)$ – phase modulation due to deformation of the projection network image on the examined surface.

Taking account of the sensitivity model of the image sensor as related to the particular colour components presented in Fig. 4, the output signals of the particular colour channels of the image sensor may be determined on the basis of (1):

$$\begin{aligned} G_{sR}(x) &= \left[G_R(x) * \frac{1}{b} \operatorname{rect} \left(\frac{x}{b} \right) \right] \frac{1}{3d} \operatorname{comb} \left[\frac{x}{3d} \right] \operatorname{rect} \left[\frac{x}{B} \right], \\ G_{sG}(x) &= \left[G_G(x) * \frac{1}{b} \operatorname{rect} \left(\frac{x}{b} \right) \right] \frac{1}{3d} \operatorname{comb} \left[\frac{x-d}{3d} \right] \operatorname{rect} \left[\frac{x}{B} \right], \\ G_{sB}(x) &= \left[G_B(x) * \frac{1}{b} \operatorname{rect} \left(\frac{x}{b} \right) \right] \frac{1}{3d} \operatorname{comb} \left[\frac{x-2d}{3d} \right] \operatorname{rect} \left[\frac{x}{B} \right]. \end{aligned} \quad (9)$$

If the frequency f_g of the images (8) is greater than the Nyquist frequency for each colour channel of the image sensor, the interpretation of the signal spectra (9), analogical to that carried out in Subsection 2.2, allows us to determine the output signals of particular colour channels of the image sensor in the form:

$$\begin{aligned} G_{sR}(x) &= \left\{ b_{0R}(x) + b_{1R}(x) \cos [2\pi(2f_{nk} - f_g)x + \Phi(x)] \right\} H, \\ G_{sG}(x) &= \left\{ b_{0G}(x) + b_{1G}(x) \cos \left[2\pi(2f_{nk} - f_g)x + \Phi(x) - \frac{2\pi f_g}{6f_{nk}} - d \frac{d\Phi(x)}{dx} \right] \right\} H, \\ G_{sB}(x) &= \left\{ b_{0B}(x) + b_{1B}(x) \cos \left[2\pi(2f_{nk} - f_g)x + \Phi(x) - \frac{4\pi f_g}{6f_{nk}} - 2d \frac{d\Phi(x)}{dx} \right] \right\} H, \end{aligned} \quad (10)$$

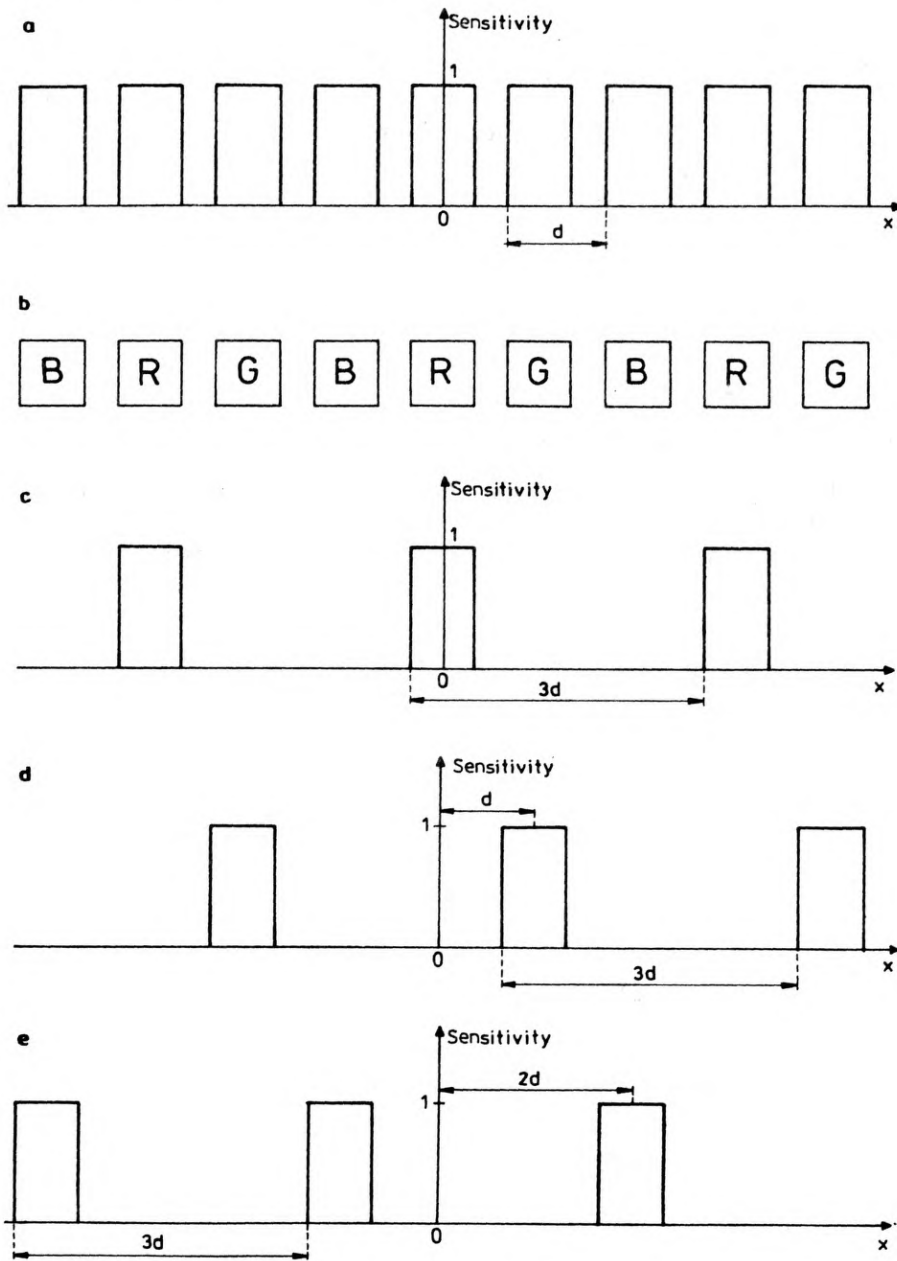


Fig. 4. Model of normalized photosensitivity of the image sensor without colour filter – a, spectral properties of primary colour stripe filter – b, model of normalized photosensitivity of the image sensor with primary colour stripe filter for the components: R – c, G – d, B – e

where:

$$H = \frac{1}{3d} \text{comb} \left(\frac{x}{3d} \right) \text{rect} \left(\frac{x}{B} \right).$$

Signals (10) represent the correctly sampled, shifted in phase fringe images of frequency $f_r = 2f_{nk} - f_g$. It should be emphasized that the period of sampling is equal to $3d$; if the coordinate (x) is expressed by the number of pixels (i), the real samples of the images $G_R(x)$, $G_G(x)$, $G_B(x)$ are located at the points $(3i)$, $(3i+1)$, $(3i+2)$. This means that the phase shifts between the images (10) may be exploited to recover the phase shifts $\Phi(3i)$. In order to recover the phase shifts of the points $(3i+1)$ and $(3i+2)$, the influence of the interpolator of the colour CCD camera with time splitting of signals on the values of signals in particular colour channels must be taken into account at these points.

3. Experimental examinations

3.1. Description of the measuring stand

In order to verify the proposed method of surface geometry measurement, a measuring stand has been built basing on commonly available elements, the scheme of which is shown in Fig. 5. A slide projector DIAPOL-150 (lamp power 150 W,

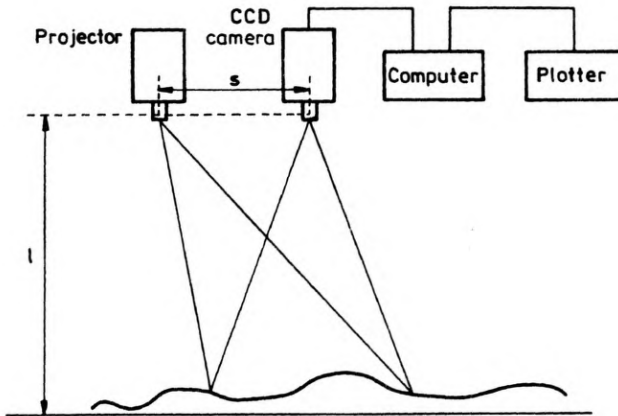


Fig. 5. Scheme of the measuring stand

objective focal length 85 mm) was used for projecting the projection network. The fringe images were observed with single-chip colour CCD camera Sony XC-711P with an objective of 35 mm focal length. The SVIST vision card working in the three-channel 8-bit A/C transducer and conjugated with the IBM PC/AT computer was exploited to record the observed images with the resolution 768×512 pixels. The recovered profiles of the examined objects were drawn on a ROLAND DXY-1100 plotter.

3.2. Results of experiments

The measuring stand described above was exploited to measure the surface geometry of two precisely produced testing objects: a ramp (foot-light) and a segment of

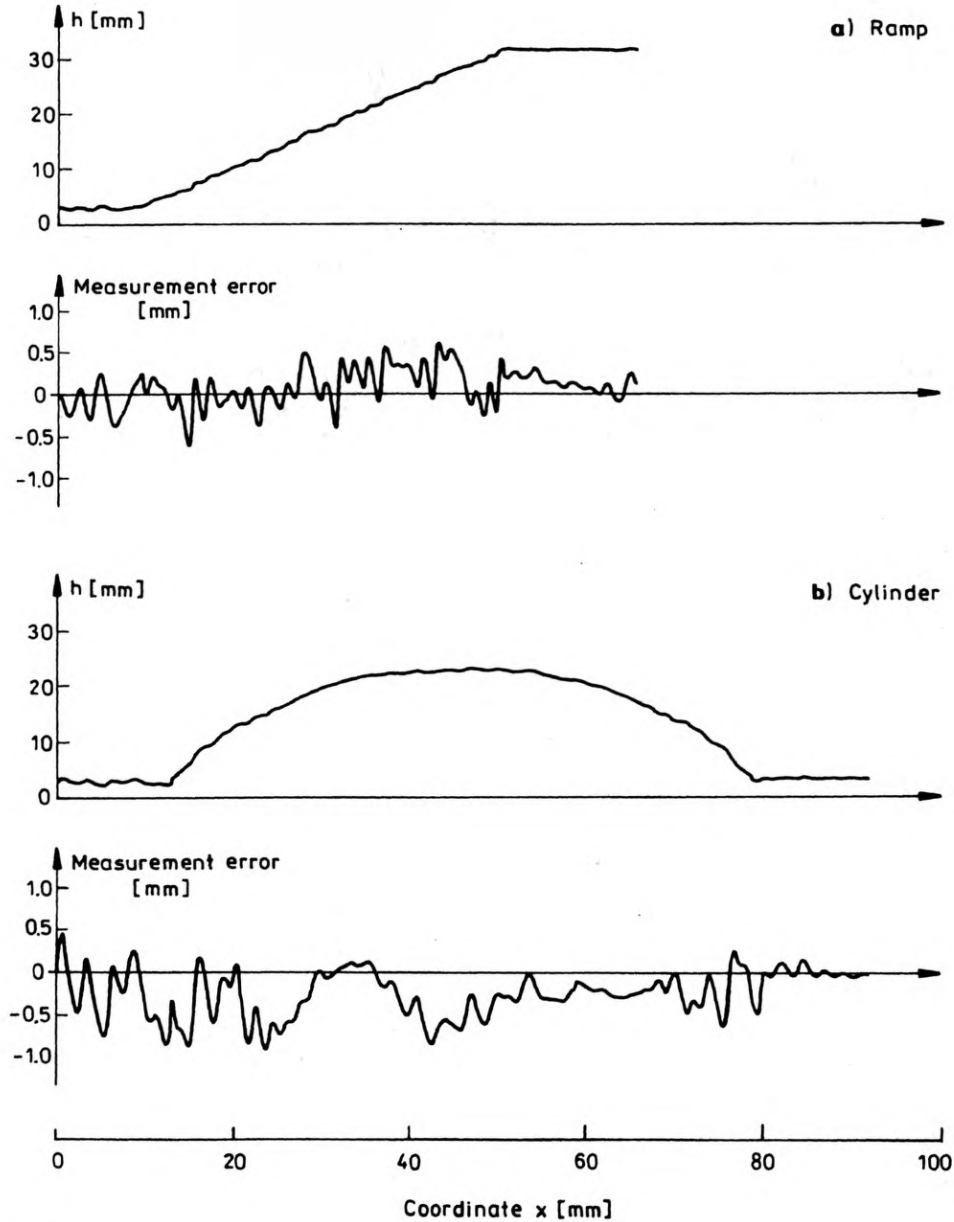


Fig. 6. Profiles and measurement errors recovered for the examined objects: **a** – ramp (foot-light), **b** – cylinder segment

cylinder. The measurements were performed on the basis of analysis of the fringe images of the reference plane and the tested objects obtained for $f_r \neq 0$. The profiles recovered with the help of the proposed method and the measurement error distributions are shown in Fig. 6. The fringe images and the intensity distribution for RGB components of the colour image of the cylinder segment are shown in Fig. 7.

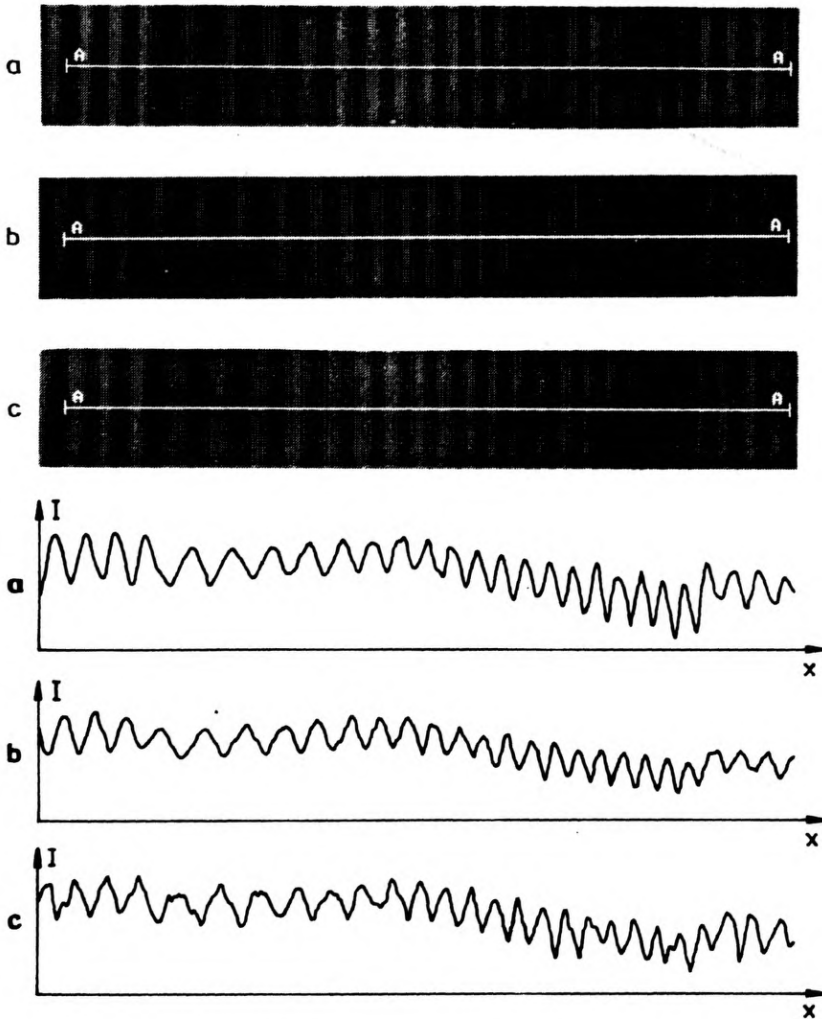


Fig. 7. Fringe images and intensity distribution of the image components in the cross-section A-A for the cylinder segment: a — component R, b — component G, c — component B

3.3. Error analysis

Errors occurring in the proposed system of surface shape measurement may be divided into two groups — errors characteristic of the method of the discrete phase change and the errors specific for the discussed method. The first group includes the following errors [9]:

- application of the projection networks of transmission profile of rectangular wave type, instead of cosine type,
- nonlinearity of detector,
- quantization error,
- optical errors (aberration, small depth of focus, *etc.*),
- mechanical vibrations,

- temperature errors,
- errors of measuring stand calibration.

The advantage of the proposed method lies in elimination of any mechanical system in the phase shifter and the due errors of phase shift determination. However, there appear some specific phase shift errors following from Eq. (10). If α_n and α_r denote nominal and real phase shifts between the images in channels R-G and G-B, respectively, the phase shift error is

$$\Delta\alpha = \alpha_r - \alpha_n = \alpha_r - \frac{2\pi}{3}. \quad (11)$$

The sources of this error are:

a) Inaccuracy of establishing $f_g = 2f_{nk}$. If the images of frequency $f_r \neq 0$ are analysed, the nominal phase shift is

$$\alpha'_n = \frac{2\pi f_g}{3 \cdot 2f_{nk}} \quad (12)$$

and the phase $\Phi(x)$ should be determined from the following dependence

$$\Phi = \arctan \left\{ \frac{1 - \cos\alpha'_n}{\sin\alpha'_n} \frac{I_R - I_B}{2I_G - I_R - I_B} \right\} \quad (13)$$

where I_R, I_G, I_B are the normalized signals in the particular colour channels.

b) The changes of phase $\Phi(x)$ between the points $(3i), (3i+1), (3i+2)$. After taking account of the first two terms in the expansion of function $\Phi(x)$ into the Taylor series around the point $(3i)$, we obtain

$$\Delta\alpha = d \frac{d\Phi(x)}{dx}. \quad (14)$$

For the measurement of phase $\Phi(x)$ by the method of discrete phase changes it is required to have information about N values of signals shifted in phase of the form

$$I_i(x) = A(x) + B(x) \cos \left[\Phi(x) + i \frac{2\pi}{N} \right], \quad i = 0 \dots N-1, \quad N \geq 3. \quad (15)$$

From Equations (10) it follows that both the d.c. components and the amplitudes of the signals shifted in phase in particular colour channels are different. This is due to different sensitivity of the CCD image sensor to RGB components and changes of colours of the examined object. This means that the signals (10) may be exploited to calculate the phase $\Phi(x)$ after their normalization. The presented measurement results were obtained by performing the following normalizations:

- sensitivity differences of the CCD image sensor to the RGB components have been compensated by a suitable selection of the dynamic ranges of the A/C transducers of the SVIST card,
- the obtained periodical signals were divided into segments of $T/2$ length

positioned between the local extremes, and next the values of signal in each of these segments were mapped into values $I \in \langle 0, 1 \rangle$.

4. Summary

In this article, a method of surface shape measurement has been proposed basing on specific periodical structure of the colour CCD image sensor. The essence of this method is similar to the idea of the surface shape measurement by the projection moire method with the discrete changes of phase. The essential difference follows from the fact that instead of precise positioning of the projection network the periodical structure of the colour CCD image sensor with colour stripe filter has been exploited to obtain the fringe images shifted in phase. This means simplification of both mechanical and optical constructions of the measurement system, similar as was the case in [4], [5], and makes possible the measurement of instantaneous state of the unstable object surfaces. The advantage of the proposed method is in replacement of the colour projection network being troublesome in production by a traditionally used and commonly available black-and-white network.

Relatively low measurement accuracy achieved follows from the fact that at the present stage of the work the main aim of the authors was only to present the theoretical basis and to demonstrate the results of application of the method to surface geometry measurement of real objects. The measurement system was built of low-precision optical and mechanical elements. The other sources of errors were: limited depth of focus of the applied optical systems, nonoptimal spectral characteristics of the projector used, errors in determination of the phase shifts between the images in particular colour channels and the differences in both the dc and ac amplitude components of these images. The said sources of errors indicate that the normalization process of the image components plays a fundamental role in creation of measurement accuracy. By selecting a suitable normalization method the measurement accuracy becomes independent of the colour of the examined object surface. In the further work aiming at improvement of the suggested method, the authors intend to concentrate their efforts on working out an optimal method of normalization.

References

- [1] SANZ J. L. C., [Ed.] *Advances in Machine Vision*, Springer-Verlag, New York 1989.
- [2] BELL B. W., KOLIOPOULOS C. L., *Opt. Lett.* 9 (1984), 171.
- [3] PATORSKI K., *Handbook of the Moire Fringe Technique*, Elsevier 1993.
- [4] WUST C., CAPSON D. W., *Machine Vision and Applications* 4 (1991), 193.
- [5] HARDING K. G., COLETTA M. P., VANDOMMELEN C. H., *SPIE* 1005 (1988), 169.
- [6] ENGELHARDT K., *Appl. Opt.* 11 (1991), 1401.
- [7] RUSIN M., *Wizyjne przetworniki optoelektroniczne* (in Polish), [Ed.] Wydawnictwa Komunikacji i Łączności, Warszawa 1990.

- [8] SZABATIN J., *Podstawy teorii sygnałów* (in Polish), [Ed.] Wydawnictwa Komunikacji i Łączności, Warszawa 1982.
- [9] ROBINSON D. W., REID G. T. [Eds.], *Interferogram Analysis*, Institute of Physics Publishing, 1993.

*Received August 9, 1993
in revised form February 7, 1994*